

“AERODYNAMIC NOISE REDUCTION FOR VARIABLE SPEED TURBINES”

P. Dunbabin¹, A. Harris¹, A. Björck², F Doorenspleet³, T. Bax³

1. Renewable Energy Systems Ltd.,

2. FFA,

3. Aerpac

Contract JOR-CT95-0045

PUBLISHABLE FINAL REPORT

January 1996 - June 1998

Research funded in part by
THE EUROPEAN COMMISSION
in the framework of the Non Nuclear Energy Programme
JOULE III

PUBLISHABLE FINAL REPORT FOR JOULE PROJECT JOR-CT95-0045
“AERODYNAMIC NOISE REDUCTION FOR VARIABLE SPEED TURBINES”

CONTENTS

CHAPTER 0 INTRODUCTION	1
CHAPTER 1 NOISE MEASUREMENTS FROM MARHKAMS VS45 TURBINE	1
1.1 MEASUREMENT PROCEDURE	1
1.2 TURBINE CONTROL.....	2
1.4 ASSESSMENT OF BROADBAND NOISE.....	2
1.4.1 Data Selection	2
1.5 RESULTS.....	2
CHAPTER 2 AERODYNAMIC ANALYSIS	4
2.1 INTRODUCTION	4
2.2 AERODYNAMIC PERFORMANCE.....	4
2.3 NOISE SENSITIVITY STUDY.....	5
2.3.1 General Models	5
2.3.2 Calculation of Aerofoil Boundary Parameters	6
2.3.3 Predictions of Noise for Different Blades	7
CHAPTER 3 ASSESSMENT OF NOISE, ENERGY PRODUCTION AND COSTS	8
3.0 INTRODUCTION	8
3.1 COSTS	8
3.2 OPTIMISATION	9
CHAPTER 4 CONCLUSIONS	9

TABLES

Table 1.01	Correlation Slopes And Regressions For Sound Power Versus Tip Speed; Normal Operation Only
Table 1.02	Slopes And Correlation Coefficients For Residuals Of Noise As A Function Of Residuals Of Angle Of Attack
Table 3.01	Predicted Noise Emission, Annual Energy Production, And Relative Cost Of Each Rotor

FIGURES

Figure 1.01	Scaled Sound Power in 315 Hz and 500 Hz Third Octave Bands Versus Log₁₀(Tip Speed)
Figure 1.02	Comparison of Normal and Manual Operation, 500 Hz Third Octave Band
Figure 2.01	A-Weighted Trailing Edge Noise from the Suction Side for Different Aerofoils (Pressure side is similar)
Figure 2.02	A-Weighted Separated Flow Noise for Different Aerofoils (Lowson’s Calculation)

- Figure 2.03** A-Weighted Separated Flow Noise for Different Aerofoils (Zero-Lift Angle Calculation)
- Figure 2.04** A-Weighted Inflow Turbulence Noise for Different Aerofoils
- Figure 2.05** Displacement Thickness and Shape Factor at $x/c=97.5\%$ for the NACA 63-618 and FX-W-84-151 Aerofoils Calculated with Free and Forced Transition at $x/c = 1\%$ on the Aerofoil Upper Side
- Figure 2.06** Displacement Thickness and Shape Factor at $x/c=97.5\%$ for the NACA 63-618 and FX-W-84-151 Aerofoils Calculated with Two Values for N in the e^N Method
- Figure 2.07** Calculated Displacement Thickness (d/c) As Function Of Angle Of Attack And Chord Position For A NACA 63-618 Airfoil. $Re=3e6$, $N=9$
- Figure 2.08** Calculated Shape Factor H (d/q) As Function Of Angle Of Attack And Chord Position For A NACA 63-618 Airfoil. $Re=3e6$, $N=9$
- Figure 3.01** Predicted Noise at Hub-Height Wind of 8 m/s, as a Function of capital Cost of Energy Per Turbine, Using Lowson's Method of Stall Noise Calculation
- Figure 3.02** Predicted Noise at Hub-Height Wind of 8 m/s, as a Function of Capital Cost of Energy per Turbine, Using Adapted BPM Method of Stall Noise Calculation

FINAL PUBLISHABLE REPORT FOR JOULE PROJECT JOR-CT95-0045
“AERODYNAMIC NOISE REDUCTION FOR VARIABLE SPEED TURBINES”

CHAPTER 0 INTRODUCTION

This project was designed to investigate aerodynamic noise emission from variable speed wind turbines. The project was divided into three parts:

- i. Comprehensive measurement and analysis of acoustic data from a variable speed turbine, the Markham's VS45. The turbine operates over a wide range of tip speeds and Reynolds numbers, and consequently should represent a good test of noise prediction theories. Furthermore, the turbine's control system can be adjusted manually to allow a wide range of pitch angles, thus allowing the collection of data taken with a wide range of angles of attack.
- ii. A theoretical analysis of predicted noise levels for a variety of blades, to identify trends with aerofoil profile, chord and twist distribution. Initially, the predictions were made with the blades twisted for optimum performance; subsequent predictions were made with the blades twisted to reduce angle of attack, to investigate the effects on noise. This study was combined with a theoretical analysis of the costs and annual energy productions of the blades.
- iii. Development of the detailed structure of a quiet and efficient blade, suitable for variable speed turbines.

The layout of the report follows these three tasks, with chapter 1 discussing the noise measurements, chapter 2 discussing the noise prediction methods, and the aerodynamic efficiency, and chapter 3 providing the overall assessment of the costs, efficiency and noise of each blade. The non-publishable report contains the absolute sound power levels of the Markham's turbine and the detailed design drawings of the scaled APX60 blade.

CHAPTER 1 NOISE MEASUREMENTS FROM MARHKAMS VS45 TURBINE

1.1 MEASUREMENT PROCEDURE

Comprehensive measurements of noise emission from the Markham's VS45 turbine were made at Kaiser-Wilhelm-Koog, Schleswig-Holstein, Germany, in May 1996. The turbine has a variable speed drive and is rated at 600 kW. The hub height is 50m, and the rotor diameter 45m. The nacelle is lined with sound absorbing material to minimise air-borne noise radiation of mechanically generated noise.

The aim of the measurements was to determine the variation of noise with tip speed, angle of attack and wind speed (independently of its effect on tip speed). The procedure used was developed for another project and is described fully in reference [1]).

Noise measurements were made using 12 ground-based microphones, placed in 30 degree intervals around a circle of radius 50m around the base of the turbine. Each microphone was mounted on reflecting boards and protected with a wind shield. The signals were amplified and recorded on synchronised Tascam tape recorders. Synchronous measurements of wind speed at 30 and 50m, wind direction, yaw position, power, rotational speed and blade pitch were also recorded onto the Tascams. The tape recorders sample at a rate of 44.1 kHz. After the experiments, selected portions of noise data were re-sampled at 20 kHz and copied to CD for further analysis.

1.2 TURBINE CONTROL

The majority of the recordings were made with the turbine operating under automatic control. However, the turbine can also be made to operate at either a fixed rotational speed or at a fixed pitch angle. Experiments were carried out using rotational speeds of 25% - 99.5% of full speed, and with pitch angles of 72 - 87 degrees (normal operation being defined by the Markham's control panel as 87 degrees of pitch). The angle of attack near the blade tip was calculated using a standard blade element program (ref [2]).

1.4 ASSESSMENT OF BROADBAND NOISE

The aim of this investigation was to use a large amount of data to ascertain the dependence of noise in different frequency bands on tip speed, angle of attack and wind speed. Since tip speed is the dominant factor in determining noise, it was decided to calculate the dependence of noise on the other variables by the method of partial residuals.

1.4.1 Data Selection

In total, 17 tapes of data were taken (approximately 34 hours' worth), although much of the data was taken during low wind speeds and had to be discarded. The remaining recordings were divided into 10s segments. Segments for which the rotor was not aligned to within ± 3 degrees of any microphone were discarded. In addition, any segments during which the yaw angle changed by more than ± 0.5 degree were discarded. However, in order to increase the number of samples taken under manual control, the alignment condition was relaxed to within ± 7 degrees of any microphone.

The recordings were sampled at 4 kHz, using filters to remove electromagnetic interference and low frequency noise. The data were then calibrated and the sound power levels in third octave bands were determined.

1.5 RESULTS

A total of 122 10s samples taken under normal operating conditions, and 171 samples taken under manual operation were analysed to establish trends with tip speed and angle of attack. It was found that:

- i. Noise is strongly correlated with tip speed in all frequency bands, the correlation coefficients (R^2) varying between 0.88 (250 Hz) and 0.61 (125 Hz). See Table 1.01.
- ii. The gradient for noise with tip speed is clearly dependent on the frequency. Figure 1.01 shows noise in the 315 Hz and 500 Hz third octave bands against $\log(\text{tip speed})$. Note that Markham's have requested that the sound power level of the machine is kept confidential, so all relevant figures have been scaled. In general, noise at frequencies below 400 Hz is less sensitive to tip speed than noise at higher frequencies. For example, at 315 Hz, the gradient is 34.15 ± 1.7 dB(A), while at 500 Hz it is 56.49 ± 2.0 dB(A). These gradients imply the following equations for noise with tip speed:

$$SPL(315_Hz) \propto U^{3.4 \pm 0.2} \quad [1.5.01]$$

$$SPL(500_Hz) \propto U^{5.6 \pm 0.2}$$

Aerodynamic theory (e.g. references [3,4,5]) indicates that aerodynamic noise is proportional to tip speed to the fifth power for all noise mechanisms.

The gradients change if data for tip speeds $< 50 \text{ ms}^{-1}$ is excluded, although the trend for higher dependence of noise on tip speed at frequencies > 315 Hz remains. A-weighted sound power levels were found to be proportional to the tip speed to the power 4.4, or 5.1 if tip speeds $< 50 \text{ ms}^{-1}$ were ignored.

- iii. Data taken under normal and manual control were plotted against tip speed, and appeared to be different in the 200 - 800 Hz third octave bands, the manually controlled samples being quieter at low to moderate tip speeds. The overall A-weighted level, however, was not significantly different. See Figure 1.02. As before, the figure has been scaled to show trends but not the absolute value of the turbine's sound power level.
- iv. Overall, the analysis provided no definite confirmation of a trend for noise with angle of attack (see Table 1.02). This is in strong contrast to theory, and also to results found by other researchers on other machines. Nonetheless, it is a valid conclusion from the data recorded.
- v. Overall, the analysis provided no definite confirmation of a trend for noise with wind speed (independently of tip speed).

CHAPTER 2 AERODYNAMIC ANALYSIS

2.1 INTRODUCTION

The aim of this task was to compare several blades in terms of their aerodynamic performance and their expected noise emission. There were four parts:

- i. analysis of aerodynamic performance of chosen blades,
- ii. description of noise prediction models, and their sensitivity to different boundary layer parameters,
- iii. description of the method of calculating boundary layer parameters, and the implications of different methods on noise prediction,
- iv. calculation of predicted noise levels for the chosen blades.

2.2 AERODYNAMIC PERFORMANCE

Aerodynamic performance calculations were made for three chord profiles, the largest having a chord equal to 141% that of the smallest. The blades were denoted:

BR1 100% chord
BR2 120% chord
BR3 85% chord.

Initially, optimum twist profiles were derived using a standard blade element code and assuming a NACA 63-618 aerofoil. A series of non-optimum twist profiles were also derived, which resulted in a lower angle of attack, at any given wind speed below rated. The reasoning was that blades with these twist profiles would be expected to produce less noise.

Additional calculations were made for the same blades with other aerofoils:

FX-W-841-151 (15.1 % thick)
NACA 63-618 (18.0 % thick)
FFA-W1-182 (18.2 % thick)
FFA-W3-211 (21.1 % thick)

As a comparison, energy yields were calculated for a commercial blade, the APX 60, which was scaled to the same diameter as the others (52m). This blade uses Delft aerofoils (DU-95-W-180).

Finally, energy yield calculations were made for blades using the NACA 63-618 aerofoil only, and operating at different rpm schedules.

2.3 NOISE SENSITIVITY STUDY

2.3.1 General Models

This section investigates some of the aspects of the noise prediction code used for this project. The code is based on a standard blade element aerodynamic program, and noise prediction algorithms taken primarily from Brooks, Pope and Marcolini (BPM), reference [6]. These algorithms apply only to the NACA 0012 aerofoil, from which they were derived. They can be extended to other aerofoils, by changing the boundary layer parameters appropriately.

The six boundary layer parameters investigated were boundary layer displacement thickness (δ^*), blade tripping, aerofoil zero-lift angle, aerofoil shape factor (H), pressure coefficient distribution and chord. These influence the noise as follows:

- i. Inflow turbulence noise depends on the variation of the aerofoil's pressure coefficient with angle of attack. As the aerofoil encounters a gust, its pressure distribution changes, giving rise to the emission of noise.
- ii. Noise due to the interaction of a turbulent boundary layer with the aerofoil's trailing edge (referred to as TBLTE noise) depends on the displacement thickness of the boundary layer.
- iii. Noise due to separated flow may be calculated by either of two methods, firstly depending on the aerofoil shape factor near the trailing edge (Lowson's method, reference [7]), or secondly on the zero-lift angle (BPM method, reference [6], adapted by Anders Björck of FFA as part of this project). Neither method has been fully validated in a wind tunnel.

A series of tests were run to illustrate the effect of changing these boundary layer parameters on each noise mechanism. The boundary layer parameters were changed either by replacing one aerofoil with another, or by changing the angle of attack. The main trends are shown in Figures 2.01-2.03:

- i. Trailing edge noise is relatively insensitive to the displacement thickness and therefore to both angle of attack and aerofoil profile. An increase in the thickness increases the linearly weighted noise level but shifts the spectrum down to lower frequencies, thus reducing the A-weighted noise level.
- ii. If Lowson's model is used, separated flow noise increases with increasing angle of attack over a range which is aerofoil dependent. The NACA 63-618 and FX-W-84-151 aerofoils are predicted to produce more separated flow noise than the FFA aerofoils. If the zero-lift angle method is used, the same trend is apparent, but the relative noisiness of different aerofoils is changed.
- iii. Using the model for inflow noise derived from [8], inflow noise is dependent on the rate of change of the aerofoil pressure coefficient with angle of attack. At moderate angles of attack, this is aerofoil dependent. Inflow noise decreases with increasing angle of attack, the degree of reduction being aerofoil dependent. The NACA 63-

618 and FX-W-84-151 aerofoils are predicted to produce less inflow noise than the FFA aerofoils.

Note that trends [ii] and [iii] offset each other.

2.3.2 Calculation of Aerofoil Boundary Parameters

Aerofoil boundary layer parameters were calculated by the program XFOIL (reference [9]). It was found that the implementation of XFOIL had very significant effects on the resulting noise prediction. Two considerations were examined; the transition method used in XFOIL, and the chordwise position at which boundary layer parameters are specified for use in the noise prediction code.

In XFOIL, the transition point can be specified at a given point (“forced” transition”), or calculated by consideration of the Tollmein-Schlichting instabilities (“free transition” or the “e^N” method). The choice affects both the displacement thickness and the aerofoil shape factor.

- i. Free transition was found to result in a greater displacement thickness, and a corresponding increase of up to 1 dB(Lin) in trailing edge noise; the increase in the A-weighted level would be lower.
- ii. The type of transition has a stronger effect on the shape factor. For the FX-W-84-151 aerofoil, the shape factor near the trailing edge is predicted to reach a value of 2.2 by $\alpha - \alpha_0 = 4.8$ degrees for the forced transition case, but to reach the same value at 8.6 degrees for the free transition case. (See Figure 2.04.) The corresponding difference in noise level could be as high as 4.6 dB(Lin). For the NACA 63-618, the difference is a maximum of 1.5 dB(Lin). Consequently, the choice of transition type is more significant for noise than the choice of aerofoil.
- iii. If “free” transition is assumed, the results can still be affected by the value of the parameter N. Comparisons were made using N=4 and N=9, the N=4 value moving the transition point closer to the leading edge. The results were less striking than the comparison between forced and free transition, but the effect was the same; for low angles of attack, the difference between different aerofoils is less important than the choice of parameter N used.
- iv. The noise prediction program was adapted to use the boundary layer parameters as estimated at the 98% chord position. FFA looked at the variation of aerofoil parameters with chordwise position. A quantity was defined as the equivalent change in angle of attack required to obtain the same change in boundary layer parameter, BL, as would be obtained were the chordwise position changed by 1%:

$$\mathbf{a}_{eq,change} = 0.01 \frac{\mathbf{d}BL}{\mathbf{d}} \bigg/ \frac{\mathbf{d}BL}{\mathbf{d}h}$$

This quantity is referred to as the "equivalent α change", and was defined for both the shape factor H and displacement thickness, \mathbf{d} .

v. For \mathbf{d} ,

- At large angles of attack, when the flow is separated, or close to separation, the angle of attack derivative is much larger than the chordwise derivative for δ^* . This means that the selection of the exact position at which the boundary layer parameters are taken is less important. For example, a change of 1% in chordwise position was found to be equivalent to a change in \mathbf{a} of 0.2 degrees.
- When the flow is attached, the situation is quite different. For the NACA-63618 aerofoil at low angles of attack, the difference in \mathbf{d} when calculated at 97.5% and 100% of the chord is roughly equivalent to the change found when the angle of attack is adjusted by 2.5 degrees.

vi. For H:

- As before, at high angles of attack (around 10 degrees), the angle of attack derivative is much larger than the chordwise derivative. However, noise is a function of H only for H values between 1.4 and 2.5. For angles of attack greater than about 6.5 degrees, H is in excess of 2.5 over the range $x/c = 97\%$ to 100% . Consequently, altering the position at which H is calculated from 97.5% to 100% has little effect on the noise at these angles of attack.
- For low to intermediate values of angle of attack, (up to 6.5 degrees), the difference in H when calculated at 97.5% and 100% of the chord may be as high as 0.5. This is roughly equivalent to the change found when the angle of attack is adjusted by 1.0 degrees. This is a very significant change.

These points are illustrated by Figures 2.05-2.07. The results constitute one of the principal findings of this project. Together, they indicate that more fundamental wind tunnel experiments are required before Lawson's model for separated flow noise can be used with confidence.

3.2.3 Predictions of Noise for Different Blades

The predictions of noise emission from the different blades showed the following:

- i. For a given wind speed and tip speed ratio, the maximum difference between predicted noise levels for the different blades was of the order of 2 dB(A).
- ii. When a blade is twisted to reduce angle of attack, the noise level may either increase or decrease, depending on the aerofoil and the dominant noise source. For the FFA aerofoils, inflow noise is generally dominant, and this is predicted to decrease with increasing angle of attack. For the NACA 63-618 and FX-W-84-151, separated flow noise is dominant (if Lawson's method is used), and this increases with increasing angle of attack.

- iii. Predictions made using Lawson's method and the zero-lift method for separated flow noise did not always agree. For example, when Lawson's method is used, predicted noise levels from the NACA 63-618 and FX-W-84-151 aerofoils are louder than those from the FFA aerofoils, while the reverse is true when the zero-lift angle method is used. For Lawson's method, the quietest blade is the BR2TV1 with the FFA-W3-211 aerofoil, while for the zero-lift method, the quietest blade is the scaled APX60 with the DU-W-95-180 aerofoil.

The model used for inflow noise used here has not been validated in a wind tunnel. In late 1997, TNO, NLR (of the Netherlands) and IAG (Germany) published full details of their new model of inflow noise (reference [10]), including a description of the numerical implementation. Their model was tested extensively in a wind tunnel, and it was found that aerofoil shape and thickness both play a part in noise emission. In general terms, thicker aerofoils produce less noise from the leading edge.

The aim of the project "Aerodynamic Noise Reduction from Wind Turbines" was to predict noise using existing techniques. Since the full details of the inflow noise model used by IAG et al. did not emerge until near the end of 1997, and since the computational work would be extensive, the new model was not included in the calculations described here. However, it is planned to ask IAG to run their model on the blades described here, as part of a UK sponsored project. Note that the questions about separated flow noise remain unanswered, as this was not part of the IAG project.

CHAPTER 3 ASSESSMENT OF NOISE, ENERGY PRODUCTION AND COSTS

3.0 INTRODUCTION

This chapter assesses the blades in relation to their predicted noise levels, costs and annual energy production. The aim is to specify the best possible blade.

3.1 COSTS

Aerpac have provided information about trends in costs for the different blades considered. The blade construction principles are described in reference [11]. The assumptions made were:

- i. Extreme loads and fatigue loads are roughly of the same importance for the blade with the shortest chord.
- ii. The relative thickness of the profiles stays constant with radial position.
- iii. Comparisons have been made for the same tip speed ratio.

The relative costs ranged from 100% (for the blade with the shortest chord) to 120% for the blade with the largest chord. Aerpac's own blade, the scaled APX60, was found to have a relative cost of 103%. In order to assess the cost-efficiency of different blades, the cost of energy should be related to the capital cost of the wind farm, not just to the cost of the blades themselves. RES estimate blade costs as 25 % of total turbine

costs, and turbine costs as 70 % of the total installation costs of a wind farm. The “capital cost of energy” is defined as the installation cost divided by the energy yield.

3.2 OPTIMISATION

For a variable speed turbine, noise is negligible at low wind speeds, while at high wind speeds, the noise emitted may be masked by background noise. It appears that the middle wind speed range is the most important for noise perception. Consequently, optimisation has been performed for a hub-height wind speed of 8ms^{-1} . The predicted noise emission, installed cost per turbine and annual energy production for each rotor were compared (Table 3.01). It was found that:

- i. If the issue of noise is ignored, the most cost effective blade in the long term is the APX blade.
- ii. If noise is included in the optimisation, the results depend on which model is used for separated flow noise.
- iii. For Lawson's method, the quietest blade is has the longest chord (BR2) and the FFA-W3-211 aerofoil. For any given site, it would be possible to replace 4 turbines using the BR3TV9, FFA-W3-211 blades with 5 turbines using BR2TV1, FFA-W3-211 blades, without increasing the overall sound power level of the wind farm. Since blade BR2 also produces more energy, the overall energy production of the wind farm could be increased by 26%, although the overall cost of the wind farm would increase by 29%. See Figure 3.01.
- iv. If noise is calculated using the zero-lift angle method, the results are very different. There is no longer any clear advantage in using blade BR2. The quietest blade is the scaled APX60, DU-95-W-180, which is also the most cost effective. See Figure 3.02.

CHAPTER 4 CONCLUSIONS

The aim of this project was to undertake a thorough investigation of blade design for variable speed wind turbines with specific emphasis being on techniques to reduce aerodynamic noise emission from the rotor. The main tasks of the project were:

- i. to perform comprehensive noise measurements on a variable speed wind turbine;
- ii. to optimise blade geometry and specify the required aerofoil characteristics for a low noise blade;
- iii. to develop aerofoil and blade designs to achieve the required aerodynamic noise and performance characteristics.

The measurements were correlated with tip speed, angle of attack, and 50m wind speed, using the method of partial residuals. The results showed that the dependence of noise on tip speed varies with the frequency of the noise, lower frequency noise (< 400 Hz) generally being less sensitive to tip speed. Correlations of residuals with angle of

attack showed no clear pattern despite the wide range of angle of attack residuals (-5 to +2 degrees). Similarly, correlations with wind speed residuals showed no clear pattern.

The theoretical study was based on the noise models of Brooks, Pope and Marcolini, and Lawson. Aerofoil boundary layer parameters were calculated using the program XFOIL. The study demonstrated that the method of calculation of these parameters has a very strong influence on the noise predictions; the most important issues being;

- i. whether free or forced boundary layer transition should be assumed
- ii. if free transition is assumed, the choice of the parameter N in the Tollmein-Schlichting equation
- iii. the chordwise position at which the aerofoil boundary layer parameters are specified.

Each of these issues can be more important than the choice of aerofoil. To clarify these questions, detailed wind tunnel measurements would be required.

Having decided on a standardised method of calculating boundary layer parameters, the effects on predicted noise were investigated. It was demonstrated that the two main noise sources, separated flow and inflow turbulence, show opposite trends with angle of attack. Furthermore, aerofoils which produce more inflow noise produce less separated flow noise and vice-versa. Predictions for a variety of blades and aerofoils at different wind speeds showed, on average, a difference of 2 dB(A) between the quietest and the noisiest, the quietest blade having a large chord (BR2) and using the FFA-W3-211 aerofoil (21.1% thick). A second set of noise predictions was run using a different model for separated flow noise (referred to as the zero-lift angle method), suggested by FFA as part of this project. The range of predictions was approximately the same as previously, but the quietest blade was found to be the APX 60, with the DU-95-W-180 aerofoil. The aerodynamic efficiencies and costs of the blades were also investigated. Taking all factors into account, the most suitable blade were a scaled version of the Aerpac APX60. The detailed design of the scaled APX 60 has been provided with the non-publishable report.

ACKNOWLEDGEMENTS

We should like to thank Udo Follrichs and colleagues of Windtest for their help with the measurements, and Ruud van Rooij of Delft University of Technology for his calculations of boundary layer parameters for the DU-95-W-180 aerofoil.

TABLE 1.01 CORRELATION SLOPES AND REGRESSIONS FOR SOUND POWER VERSUS TIP SPEED; NORMAL OPERATION ONLY

Frequency	Tip Speed < 50 ms ⁻¹		Tip Speed >= 50 ms ⁻¹		All Data		
	Slope	R ²	Slope	R ²	Slope	Std Error	R ²
125	8.96	0.04	31.88	0.48	38.55	2.265	0.71
160	5.73	0.01	35.79	0.53	36.83	2.203	0.70
200	6.91	0.08	39.95	0.78	28.65	1.630	0.72
250	19.86	0.40	42.75	0.79	43.57	1.439	0.88
315	77.12	0.83	41.79	0.80	34.15	1.655	0.78
400	23.16	0.32	45.70	0.47	54.45	3.132	0.72
500	20.47	0.31	66.56	0.85	56.49	1.972	0.87
630	33.38	0.38	49.39	0.76	45.88	1.828	0.84
800	19.98	0.46	55.68	0.69	48.18	2.370	0.77
1000	-7.27	0.08	54.02	0.74	39.51	2.357	0.70
1250	43.49	0.58	43.56	0.67	30.51	2.247	0.61
1600	15.07	0.68	70.51	0.77	53.67	2.740	0.76
A_wtd	27.07	0.66	51.13	0.79	44.30	1.72	0.85

TABLE 1.02 SLOPES AND CORRELATION COEFFICIENTS FOR RESIDUALS OF NOISE AS A FUNCTION OF RESIDUALS OF ANGLE OF ATTACK

Frequency / Hz	Regression using all tip speeds together	
	Gradient dB(A) / log ₁₀ (degrees)	Correlation Coefficient R ²
< 114	-1.61	0.60
125	0.60	0.42
160	0.90	0.38
200	0.10	0.01
250	1.08	0.65
315	-0.18	0.06
400	0.62	0.40
500	0.55	0.25
630	0.20	0.13
800	0.15	0.05
1k	0.09	0.02
1.25k	-0.45	0.20
1.6k	0.63	0.42
All A-Weighted	0.21	0.15

TABLE 3.01 PREDICTED NOISE EMISSION, ANNUAL ENERGY PRODUCTION, AND RE

Case Number	Blade	Aerofoil	Wind Speed / ms^{-1}	Energy Yield / MWh	Predicted Sound Power (Lowson's Method) / dB(A)	Predicted Sound Power (Zero-Lift Angle Method) / dB(A)	Cost of Blades BR3TV7=100%	Installed Turbine 10
66	BR3TV8	FFA-W1-182	8	2701	101.59	101.8626	100	
218	BR3TV8	FFA-W3-211	8	2701	101.41	101.9401	100	
72	BR3TV9	NACA 63618	8	2683	102.19	101.3036	100	
76	BR3TV9	FX-W-84-151	8	2683	102.07	101.2431	100	
222	BR3TV9	FFA-W3-211	8	2683	101.35	101.9121	100	
80	BR3TV9	FFA-W1-182	8	2683	101.45	101.8869	100	
48	BR3TV7	FX-W-84-151	8	2707	101.54	100.3175	100	
44	BR3TV7	NACA 63618	8	2707	101.66	100.4347	100	
210	BR3TV7	FFA-W3-211	8	2707	101.48	101.9158	100	
62	BR3TV8	FX-W-84-151	8	2701	101.94	100.9454	100	
58	BR3TV8	NACA 63618	8	2701	101.90	100.8538	100	
52	BR3TV7	FFA-W1-182	8	2707	101.85	101.7915	100	
237	APX	DU-95-W-180	8	2722	101.46	99.73943	103	
6	BR1TV1	FX-W-84-151	8	2737	101.58	100.6473	109	
20	BR1TV2	FFA-W1-182	8	2731	100.92	101.4864	109	
24	BR1TV2	FX-W-84-151	8	2731	101.67	100.4609	109	
2	BR1TV1	NACA 63618	8	2737	101.71	100.7158	109	
16	BR1TV2	NACA 63618	8	2731	101.86	100.9914	109	
214	BR1TV2	FFA-W3-211	8	2731	100.81	101.4668	109	
202	BR1TV1	FFA-W3-211	8	2737	100.87	101.506	109	
10	BR1TV1	FFA-W1-182	8	2737	101.05	101.4917	109	
38	BR2TV1	FFA-W1-182	8	2736	100.24	100.8925	120	
206	BR2TV1	FFA-W3-211	8	2736	100.16	100.8415	120	
34	BR2TV1	FX-W-84-151	8	2736	101.02	100.4609	120	
30	BR2TV1	NACA 63618	8	2736	101.21	100.4245	120	

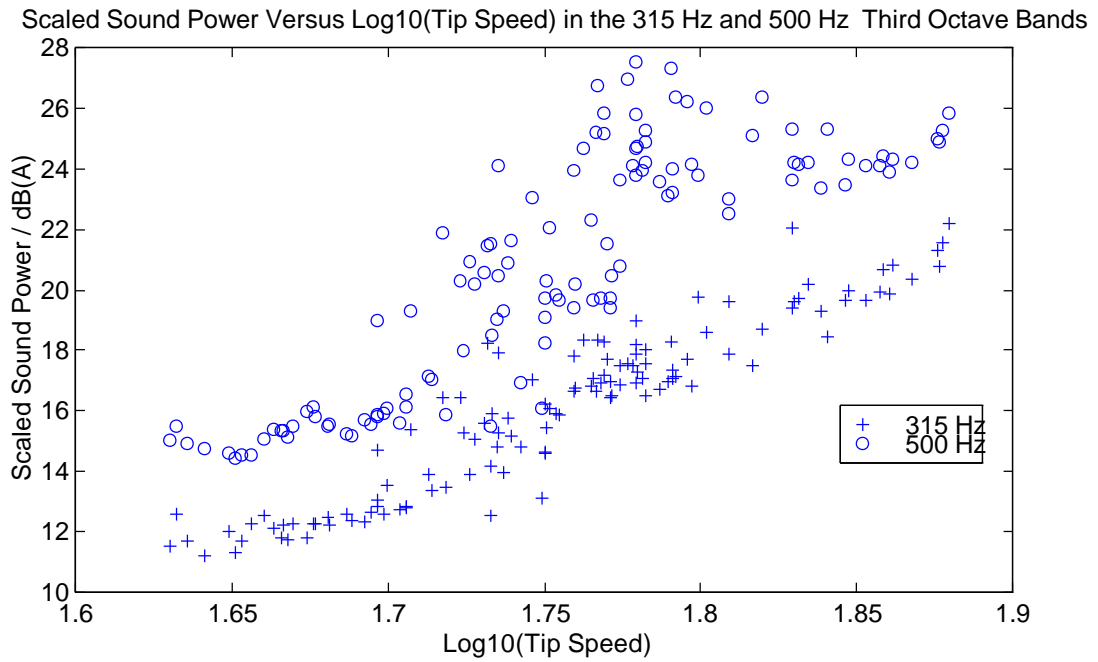


Figure 1.01 Scaled Sound Power in 315 Hz and 500 Hz Third Octave Bands Versus Log10(Tip Speed)

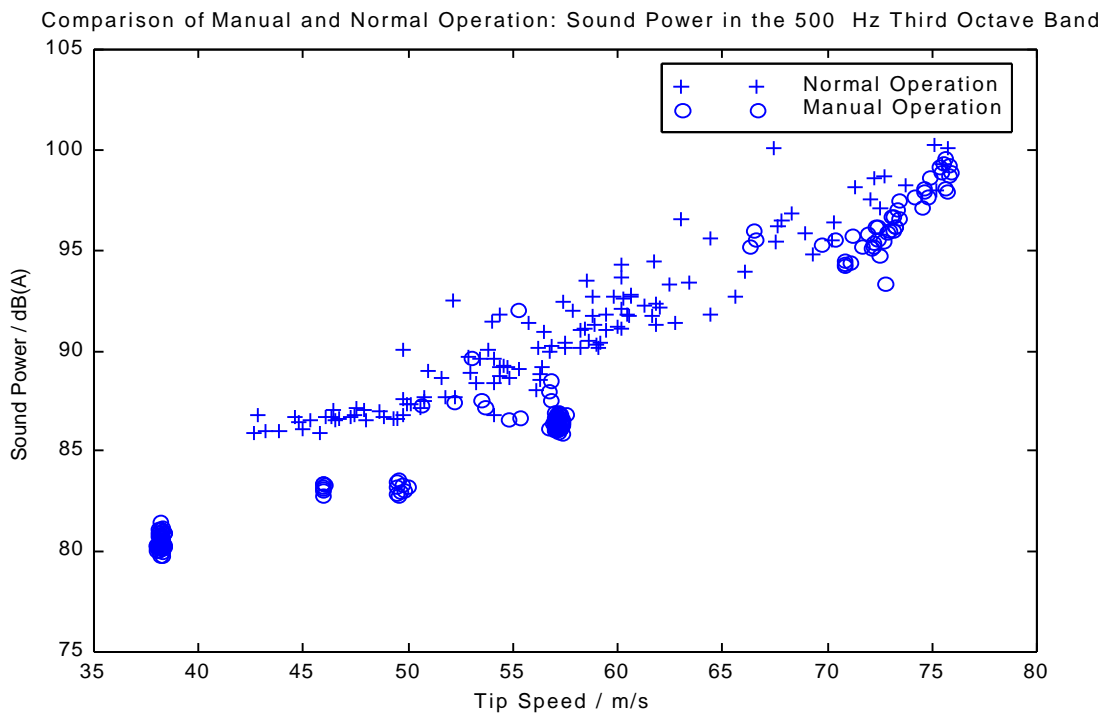
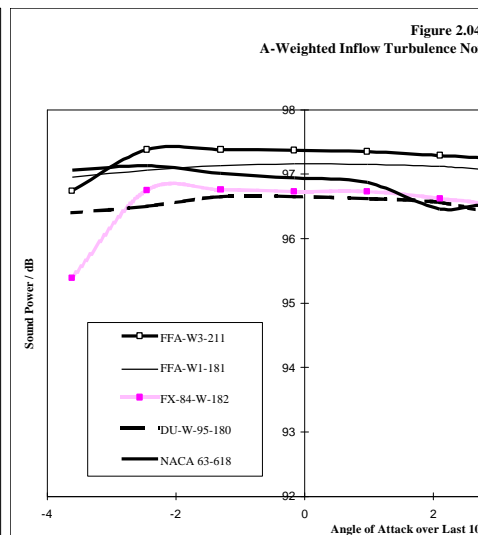
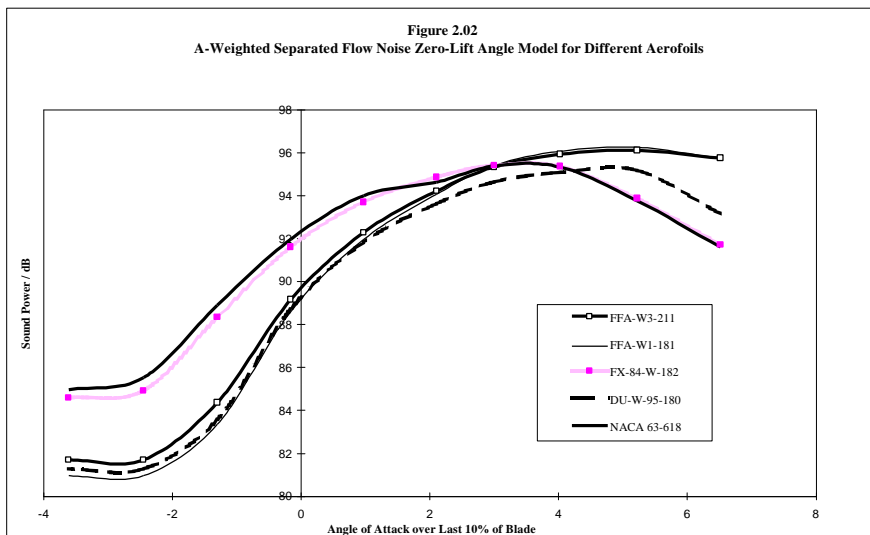
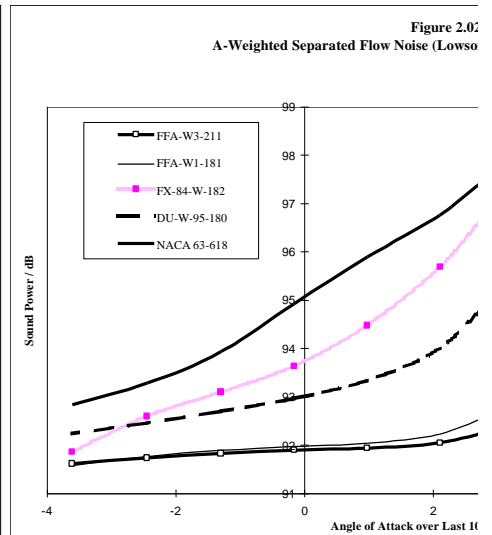
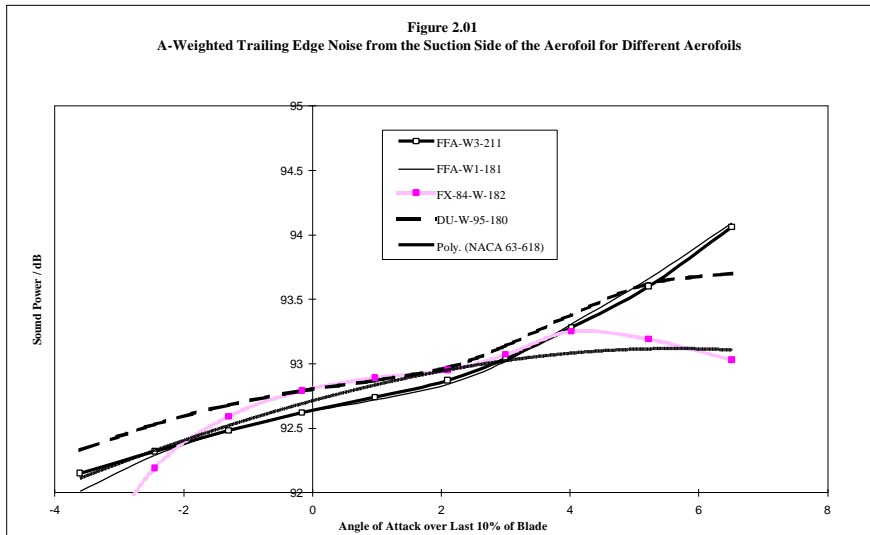


Figure 1.02 Comparison of Normal and Manual Operation, 500 Hz Third Octave Band



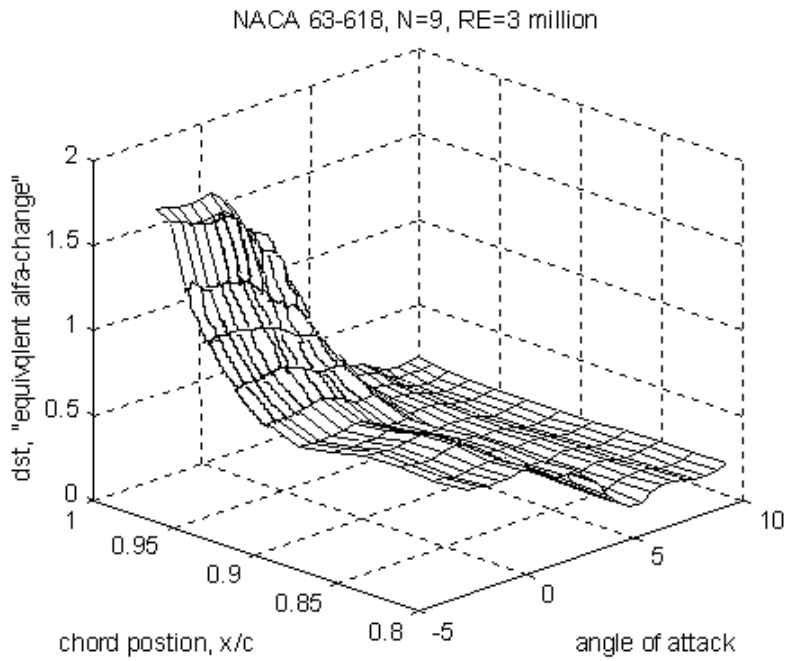


Figure 2.07 Calculated Displacement Thickness (d/c) As Function Of Angle Of Attack And Chord Position For A NACA 63-618 Airfoil. $Re=3e6$, $N=9$

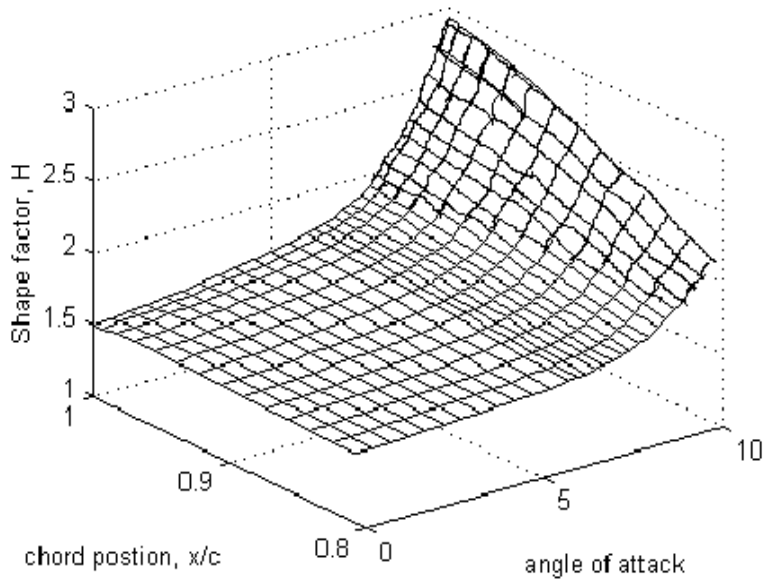
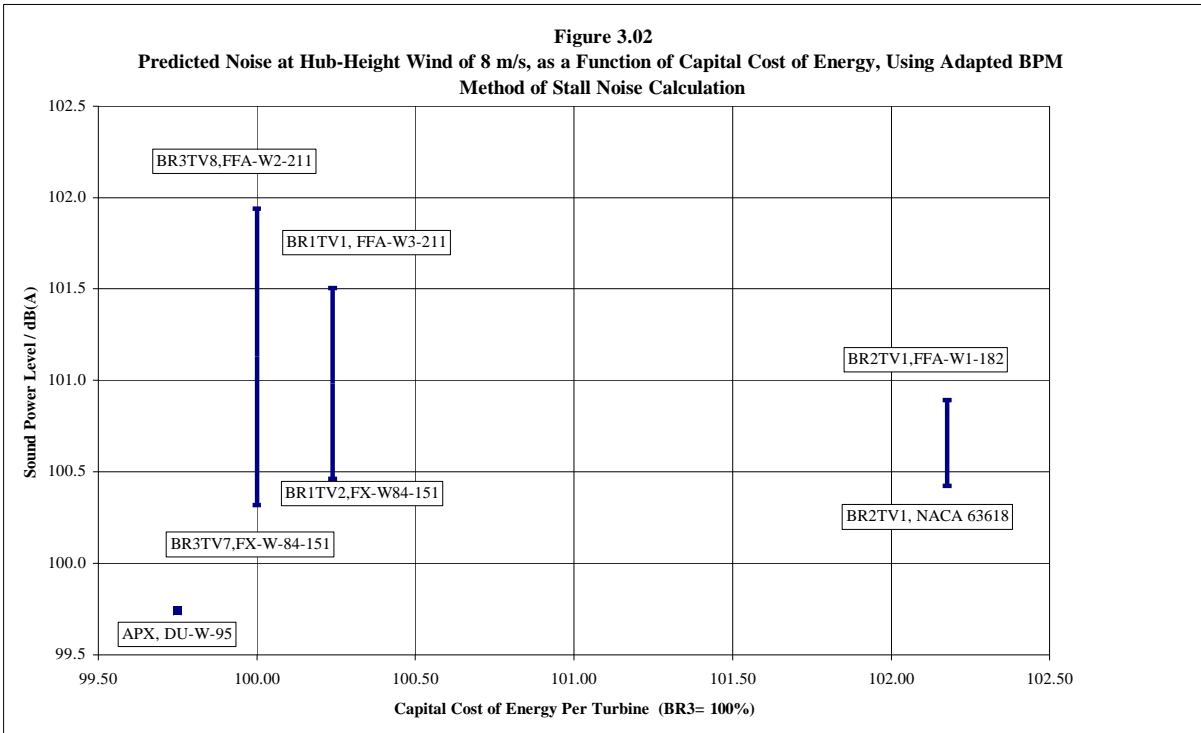
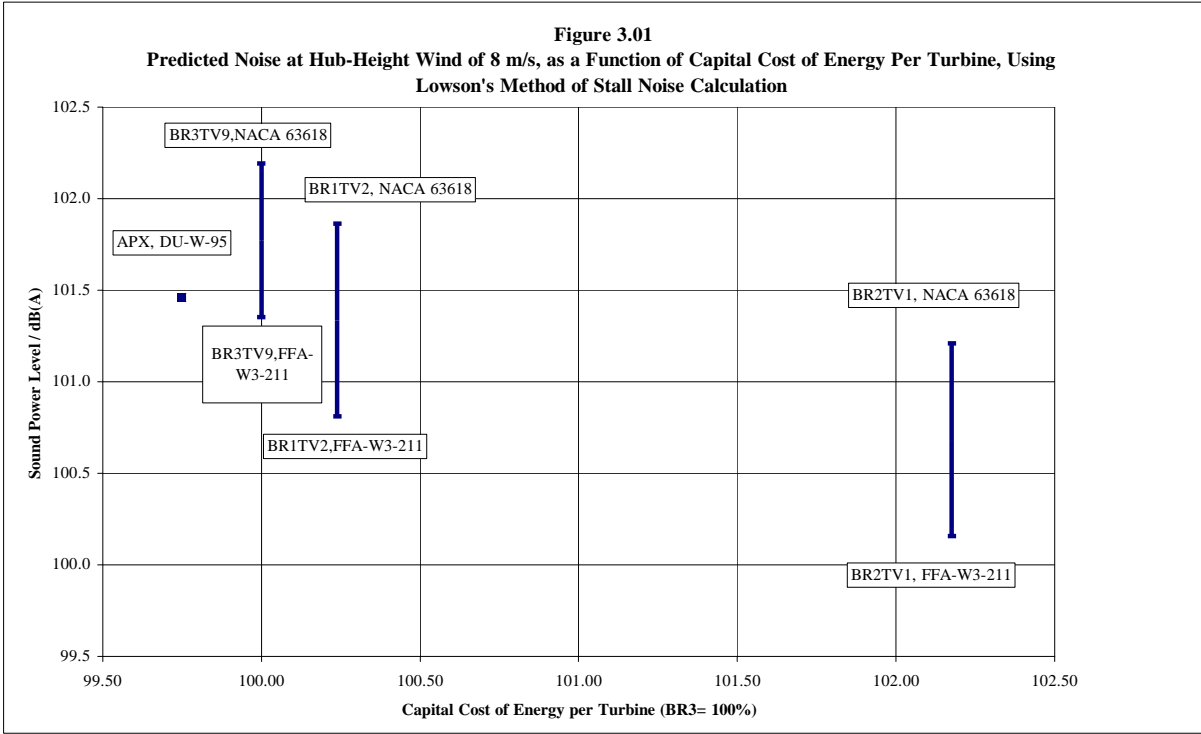


Figure 2.08 Calculated Shape Parameter H (d/q) As Function Of Angle Of Attack And Chord Position For A NACA 63-618 Airfoil. $Re=3e6$, $N=9$



REFERENCES

- [1] "A New Approach to Wind Turbine Noise Measurement", Lawson, J., Dunbabin, P., Bullmore, A, Paper P11.10, 1996 European Wind Energy Conference, pp 817 - 820
- [2] "An Experimental and Theoretical Study of Horizontal Axis Wind Turbines", M. B. Anderson, PhD thesis, University of Cambridge, 1981
- [3] "Wind Turbine Noise", Wagner, S., Bareiß, R. & Guidati, G, Published by Springer Verlag, Heidelberg, 1996 (ISBN 3-540-60592-4 & 0-387-60592-4), section 4.3.2
- [4] "Design Prediction Model for Wind Turbine Noise: 1. Basic Aerodynamic and Acoustic Models", Lawson, M.V. & Fiddes, S.P., Flow Solutions report 93/06, 15/11/93, Published by ETSU, number W/13/00317/00/00.
- [5] "Design Prediction Model for Wind Turbine Noise: 3. Inflow Turbulence Study and Full Model Integration" Lawson, M.V. & Fiddes, S.P., Flow Solutions report 94/02 2/5/94
- [6] "Airfoil Self Noise and Its Prediction", Brooks, T.F. Pope, D.S, & Marcolini, M, NASA publication 1218, June '89
- [7] "Design Prediction Model for Wind Turbine Noise: 1. Basic Aerodynamic and Acoustic Models", Lawson, M.V. & Fiddes, S.P., Flow Solutions report 93/06, 15/11/93, Published by ETSU, number W/13/00317/00/00.
- [8] "Wind Turbine Noise", P. Dunbabin, PhD Thesis, University of Edinburgh, 1994
- [9] "XFOIL, An Analysis and Design System for Low Reynolds Number Airfoils", Mark Drela, MIT Department of Aeronautics and Astronautics, Lecture Notes in Engineering 54, Notre Dame, Springer Verlag, June 1989
- [10] "Simulation and Measurement of Inflow Turbulence Noise on Airfoils", Guidati, G., Bareiß, R., Wagner, S., Dassen, T., & Parchen, R., Paper submitted to the AIAA, 1997, work supported by CEC under contract JOR3-CT95-0083.
- [11] "The Development of Rotor Blades for Megawatt-Size Stall Regulated Wind Turbines", Doorenspleet, F. & Anderson, C.G., Aerpac BV, The Netherlands, Published as Paper 07.6 EUWEC 1996, Göteborg 1996